

## ON THE USE OF HETEROGENEOUS, WIRELESS SENSOR NETWORKS FOR DAMAGE ASSESSMENT IN BRIDGES UNDER UNKNOWN EXCITATIONS

T. Kijewski-Correa, S. Su, E. Abittan, P.J. Antsaklis  
 University of Notre Dame, Notre Dame, IN 46556 USA  
[tkijewsk@nd.edu](mailto:tkijewsk@nd.edu), [ssu@nd.edu](mailto:ssu@nd.edu), [abittan.1@nd.edu](mailto:abittan.1@nd.edu), [antsaklis.1@nd.edu](mailto:antsaklis.1@nd.edu)

### Abstract

A multi-scale wireless sensor network was previously introduced by the authors and their collaborators, integrating data from a heterogeneous sensor array for a more robust and effective approach to damage detection. This multi-scale network concept was developed to improve power efficiency, minimize packet loss and latency, and eliminate synchronization issues through the use of decentralized analysis schemes and the activation of sub-networks only in the vicinity of suspected damage. Specific focus is given here to the vibration-based damage detection algorithms operating in the lower tier or micro-network, which do not require knowledge of the system input. Two approaches for decentralized system identification are evaluated: Method 1 uses residuals, while Method 2 derives its damage sensitive feature directly from regressive coefficients. Both use heterogeneous sensor measurements in lieu of measured inputs to the system. The utility of data fusion, spatially and temporally, within the upper tier or meso-network is also demonstrated as a means of reducing both false positives and false negatives.

### Introduction

Given the burdens associated with inspection and maintenance of Civil Infrastructure, the development of effective, automated damage diagnosis techniques, including the sensor technologies that support them, has become a major research need. While advances in wireless sensor networks have demonstrated their potential to provide continuous structural response data to assess health (e.g., Straser and Kiremidjian, 1998; Lynch *et al.*, 2003), issues including network lifetime and stability, damage detection reliability, and overall effectiveness when using low-cost sensors must be realistically addressed. This prompted the authors and their collaborators to introduce a multi-scale wireless sensor network for bridges that utilizes a heterogeneous sensor array (Kijewski-Correa *et al.*, 2005).

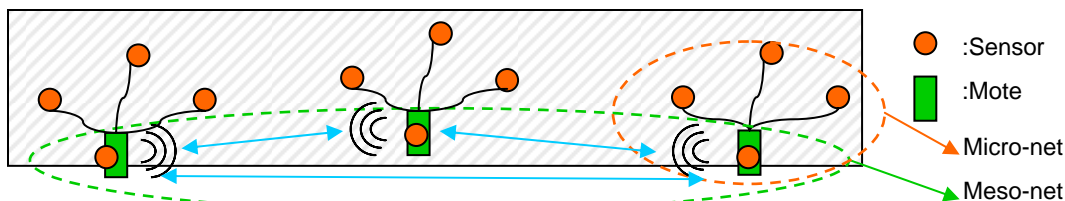


**Figure 1. Two-tiered architecture of multi-scale wireless sensor network.**

Both the network architecture and hardware details were reported previously (Kijewski-Correa *et al.*, 2005; 2006) and are excluded here for brevity, as this study now focuses on the damage detection algorithms embedded in the network; however, some pertinent details of the network concept are briefly summarized in Table 1. As shown in Figure 1, the network is multi-tiered in nature, beginning first with the micro-net of Mica motes equipped with accelerometers and wired to a series of strain gauges. All damage detection is conducted in a decentralized framework using the mote's available computational resources. These interface with surrounding motes to form a meso-net, where local data fusion of binary damage reports is performed to enhance detection capability. The use of local processing and transmission of limited information to the upper tiers of the network eliminates synchronization issues and conserves power.

It is assumed that the excitation source is not measured. This fact and the reliance on the embedded processing of the wireless network constrain the algorithms employed. However, the network’s event-synchronization via the Restricted Input Network Activation Scheme (RINAS) helps to somewhat constrain the inputs to the system (Kijewski-Correa *et al.*, 2006). The network is essentially dormant until vehicle passage and environmental conditions match the user’s specifications, at which time RINAS triggers the network from the macro-node (or Stargate). This approach helps to significantly reduce the reference pool for damage detection. It will be further demonstrated in this study that such signal-based, time-series methods, operating within the micro-net’s heterogeneous sensor arrays, can work within these constraints to deliver a reliable detection algorithm. Two approaches for decentralized system identification are evaluated: Method 1 is residual-based approach, while Method 2 derives its damage sensitive feature from the coefficients of a regressive model. This paper will now introduce and demonstrate the performance of each method, as well as the merits of data fusion in the meso-nets.

FEATURE	SELECTION	ADVANTAGE
Sensors	Acceleration, Strain	More sensitive to damage when combined
Excitation	Ambient, Event Triggering	No disruption of operation, maximize lifetime
Network Architecture	Two-tiered, wireless globally, wired locally	Low power, low latency, scalable
Damage Detection	Decentralized, low order, time-series, local fusion	Easily embedded, event synchronized, more reliable
Variability (Operational, Environmental)	Statistical Significance, Restrict Network Activation	Reduce false positives, reduce reference pool size
Power Consumption	Decentralized identification, event triggering, exploit sub-networks	Maximize battery life

**Table 1. Overview of key features of proposed multi-scale wireless sensor network.**

### Overview of Signal-Based Detection Schemes

Damage estimation methods based on the vibration data can be classified into two groups, based on whether an explicit structural model is involved: model-based methods and signal-based methods (Zou *et al.*, 2000). Most usual techniques to this problem belong to the first group, building upon traditional system identification approaches (Doebeling and Farrar, 1999) by relating changes in modal parameters to changes in the physical properties of the structure. This study focuses on signal-based methods adapted to a heterogeneous format suitable for decentralized system identification. As this does not impose a structural model on the system, it is very simple and attractive for automated monitoring. One of the most recognized signal-based detection schemes is the two-stage AR-ARX method developed at Los Alamos National Laboratory (LANL) (Sohn and Farrar, 2001). In this study, similar signal-based detection schemes will be explored; however, exploiting heterogeneous sensor arrays within the micro-net, as it has been shown that the combination of strain and acceleration is superior for damage detection in comparison with the use of either alone (Law *et al.*, 2005).

First, the case for a heterogeneous approach to damage detection is established. Consider a bridge represented by  $Y = G U$ , where the system transfer function matrix  $G$  under input  $U$ , yields output  $Y$ , comprised of two types of measurements:  $Y_1$  and  $Y_2$ . A noted change in the outputs could be the result of a change in the system or the inputs to it. As changes in the system may not be associated with damage but rather the result of sensor/model error and environmental variabilities, a probabilistic framework is necessary, as discussed previously (see Table 1). However, the more pressing concern is the fact that

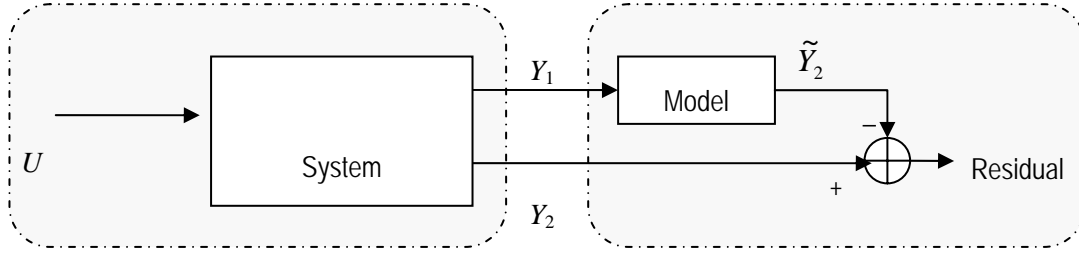


**Figure 2. Surrogate input concept operating in the micro-net.**

inputs to the system, e.g., traffic, wind, earthquake, generally are not measured, though they can be restricted by RINAS or other means. Therefore, the traditional input-output model cannot be used to monitor changes in the system. It is proposed here to circumvent this issue by exploiting the heterogeneous sensor array and using one of the measured system outputs as a “surrogate input” to the damage detection model. Two proposed heterogeneous modeling schemes building on this premise are now introduced, each with its own damage sensitive feature (DSF).

*Method 1: DSF by Residuals*

The first method builds on this transfer function concept through residual monitoring Abittan (2006), as shown in Figure 2. The form of the model is rather inconsequential and can be simply viewed as an empirical transfer function relating the two system outputs, executed in the time domain to reduce the number of operations and avoid signal processing issues associated with the Fourier transform. As such, a discrete autoregressive moving averages (ARMA) time-domain model is given by:

$$\tilde{Y}_2(n) = \tilde{H}_{21}(z) \cdot Y_1(z) = \sum_{k=0}^{Na} \alpha_k \cdot Y_1(n-k) - \sum_{j=1}^{Nb} \beta_j \cdot \tilde{Y}_2(n-j), \forall n > Nb \quad (1)$$

However, in the examples which follow, a simplified 4<sup>th</sup> order autoregressive (AR) model is introduced ( $\beta_k = 0, k=1:Nb$ ) retaining acceleration as the input ( $Y_1$ ) and strain as the output ( $Y_2$ ). Note the model order is kept intentionally low for easy embedment in the wireless platform. Deviations between the actual measured strain ( $Y_2$ ) and the predicted strain ( $\tilde{Y}_2$ ) based on simultaneously acquired acceleration data ( $Y_1$ ), all  $N$  points long, are described by the residual, whose average value is given by

$$R = \frac{1}{N} \sum_{n=\max(Na, Nb)}^N r(n) = \frac{1}{N} \sum_{n=\max(Na, Nb)}^N (Y_2(n) - \tilde{Y}_2(n)) = \frac{1}{N} \sum_{n=4}^N \left( Y_2(n) - \left( \sum_{k=0}^4 \alpha_k \cdot Y_1(n-k) \right) \right) \quad (2)$$

$R$  is retained as the damage sensitive feature and is referenced to a dynamic threshold,  $h$ , that is a linear function of the system input (acceleration) to account for the variable amplitude of response.

$$h = \lambda \cdot \text{avg} [Y_1(n)] \quad (3)$$

The scaling parameter  $\lambda$  can be derived empirically from an undamaged reference pool according to the allowable false positive rate set by the user. Damage is identified locally at a node if  $|R| > h$ .

### Method 2: DSF by Coefficients

In Method 2, the outputs  $Y_1$  and  $Y_2$  (Fig. 2) are respectively assigned to the acceleration and strain, the reverse of the convention adopted in Method 1. To avoid the need for a dynamic threshold, all simultaneously acquired acceleration and strain signals are demeaned and normalized by their standard deviation (Sohn and Farrar, 2001). Each resulting strain and acceleration data pair ( $Y_1$ ,  $Y_2$ ) is then fit by the following model using the simultaneously measured strain ( $Y_1$ ) and acceleration ( $Y_2$ ) data:

$$\tilde{Y}_2(n) = \sum_{k=1}^{Na} \alpha_k \cdot Y_1(n-k) - \sum_{j=1}^{Nb} \beta_j \cdot Y_2(n-j), \forall n > Nb \quad (4)$$

Note, in contrast with Equation 1, past observations of the output  $Y_2$  are used, as opposed to past predictions, and model orders are selected using the Akaike Information Criterion (AIC). Interestingly, at locations where strain levels are very small and engulfed in noise, the method essentially reduces to an ARX model, akin to that adopted by Sohn and Farrar (2001). The advantages of the model in Equation 4 were demonstrated previously in Kijewski-Correa *et al.* (2006), using the DSF of Sohn and Farrar (2001).

A new DSF is now proposed to better exploit the most prominent model coefficients, as opposed to using a specific coefficient (Nair *et al.*, 2006). The DSF depends on a reference pool of acceleration/strain pairs from the bridge in its initial, preferably undamaged, condition. This pool should encompass all envisioned operational and environmental conditions for the bridge. Each of these reference signal pairs are fit by the model in Equation 4 and stored in the reference database (ref). The DSF is defined as model coefficient that is largest relative to the values stored in the reference database:

$$DSF = \max \left[ \left. \frac{\left| \alpha_k - \text{avg}_{ref}[\alpha_k] \right|}{\text{std}_{ref}[\alpha_k]} \right|_{k=1:Na}, \left. \frac{\left| \beta_j - \text{avg}_{ref}[\beta_j] \right|}{\text{std}_{ref}[\beta_j]} \right|_{j=1:Nb} \right] \quad (5)$$

Subsequent DSF values are then compared to those generated from the reference pool itself and statistically significant differences are attributed to damage of the system. As demonstrated later in this paper, a Gaussian model can generally be applied to represent the DSF values of the reference pool, allowing the user to specify a desired percentile, e.g., 95%, for the statistical significance test. Therefore, let  $DSF_p$  represent the DSF from the reference pool at percentile  $P$ . Then damage is indicated with  $P$ -percent certainty whenever a future DSF value satisfies the following inequality:  $DSF > DSF_p$ .

### Performance Verification

To demonstrate the performance of these two signal-based methods, a finite element model (FEM) was used to generate a suite of undamaged and damaged cantilever beams under various inputs. Each FEM node is assumed to have only two degrees-of-freedom (DOFs): transverse displacement and rotation. Outputs of strain and acceleration are simulated at four locations along the beam length, as shown in Figure 3. Inputs are imparted at the free-end (Point D). Damage is introduced to the beam at a location  $L_D$  from the fixed end by a transverse cut of width  $W_D$ , symmetrically imparted so that the damage can be specified by the percentage ( $p$ ) of the beam's width ( $W$ ) that is compromised.

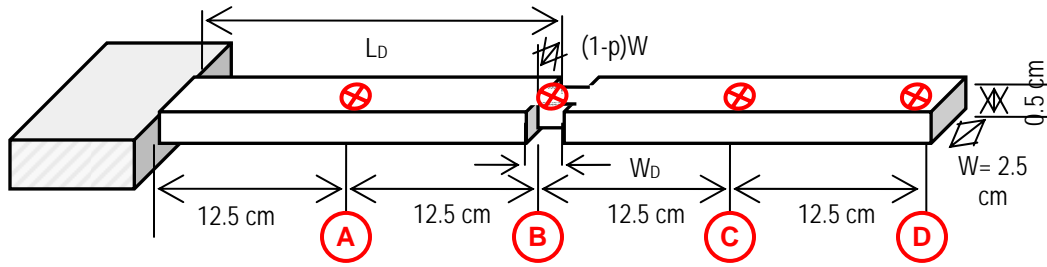


**Figure 3. Rendering of simulated beam model (not to scale).**

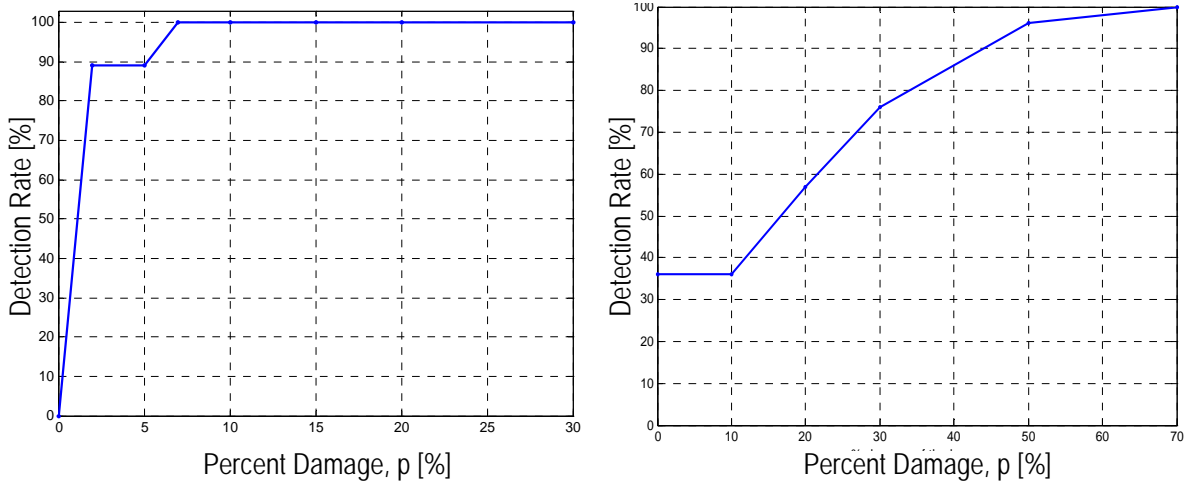


**Figure 4. Fault detection rate for Method 1 without and with noise (right).**

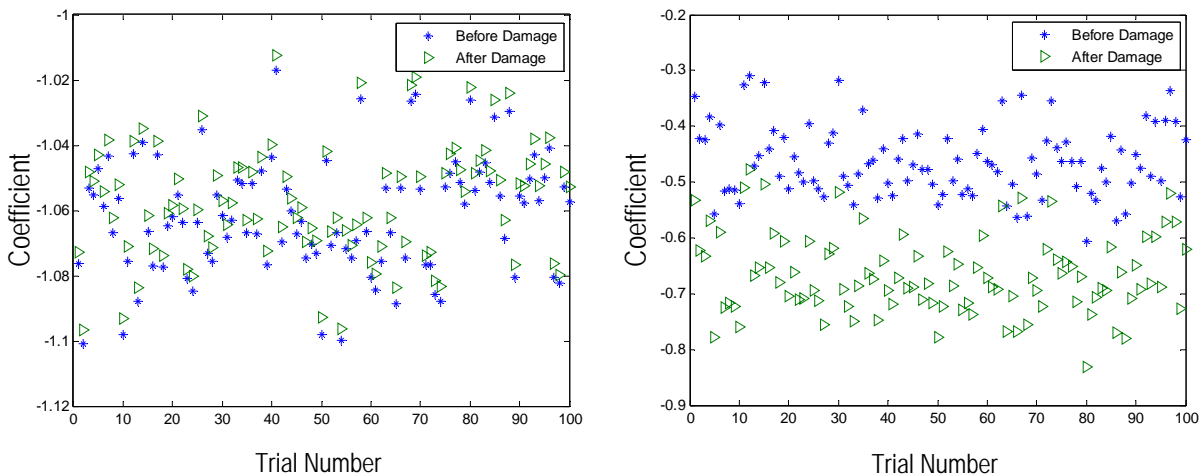


**Figure 5. Comparison of model coefficients at Location B before (◆) and after (▷) damage: first coefficient (left) vs. most prominent coefficient.**

*Method 1: DSF by Residuals*

The first example demonstrates the performance of the residual-based approach using the aforementioned thin beam model with  $W_D$  of 1 cm and  $L_D$  of 24 cm (approximate midspan). An impulsive loading is applied at point D, randomized in amplitude and duration for 100 independent trials. Figure 4

demonstrates the performance of the proposed method in a noise-free environment using acceleration and strain data recorded at point D. Note that very low levels of damage can be detected with 100% repeatability and there is no incidence of a false positive. As expected, in the presence of noise (SNR = 100:1), both the incidence of false positives increases as does the damage level required before 100% detection rate can be achieved. The performance degradation in the presence of noise is more pronounced at locations such as D due to the relatively lower amplitude of the strain response at this location. Performance improves in regions of higher strain.

#### *Method 2: DSF by Coefficients*

To demonstrate the performance of Method 2, 100 acceleration and surface strain time history pairs are generated at each measurement point by driving the model with independent Gaussian white noise excitations. These records form the reference data pool that will be used to determine a threshold value on the DSF. A Gaussian model is generally adopted to represent the empirical distribution on the DSF, since any deviations in the tails are less pronounced for the upper values of the DSF actually used for damage detection. Thus, a 97.5% one-sided Gaussian confidence interval is adopted as the damage threshold.

Various degrees of damage are now explored for cuts introduced at  $L_B = 18.75$  cm, midway between points A and B of the beam. The width of the cut is ( $W_D$ ) is 5% of the total length of the beam (2.5 cm). Each damaged simulation is repeated 10 times to explore the detection rate over repeated trials. Damage detection results are shown in Table 2, where bold faced values indicate that damage was detected. Results are compared to the approach by Nair *et al.* (2006). A number of important observations can be made regarding Method 2:

1. Damage levels of 30% or more can be identified reliably at all measurement locations, and all damage levels can be detected reliably at locations A and B. This can be explained by the fact that slight damages are more difficult to detect further from the damage origin and this strain-driven approach performs best in regions of high strain, typical of actual damage locations.
2. DSF values increase with damage level and proximity to the damage location. As expected, the DSF takes on its largest values at points A and B, demonstrating the localization capability.
3. Damage detection capability within the heterogeneous framework is improved in comparison to homogeneous methods such as Nair *et al.* (2006), as shown here, and Sohn and Farrar (2001), as discussed in Kijewski-Correa *et al.* (2006). This demonstrates the enhanced detection capabilities of a heterogeneous approach for minor levels of damage. This improved performance is also attributed to the choice of an “adaptive” DSF. Recall the DSF in Equation 5 exploits the most prominent model coefficient, whether it is associated with acceleration or strain, in contrast to using a pre-defined model coefficient. As shown by the simulation result in Figure 5 ( $p=10\%$ ), the first coefficient is not always most sensitive to damage for the model in Equation 4.
4. Incidence of false positives for this approach is negligible in comparison to the detection rate.
5. Improved signal reconstruction: residuals associated with Equation 4 are smaller than those generated by a homogeneous autoregressive model (acceleration only) of the same order.
6. Reduced computational burden/memory requirements: since only model coefficients are retained for the DSF, the size of the reference pool and the number of computations are minimized, an issue that has proved problematic in other applications (Lynch *et al.*, 2004).

#### *Data Fusion at the Meso-Net*

One of the major advantages of the multi-scale network concept is the ability to fuse data locally to enhance detection capabilities and reduce the probability of false positives. At each node, either of the aforementioned detection schemes can generate a local binary report  $B$ , ( $0 =$  no damage,  $1 =$  damage).

	POINT A						POINT B					
	Nair <i>et al.</i> (2006)			Method 2			Nair <i>et al.</i> (2006)			Method 2		
Threshold	(-0.49, -0.3)			DSF <sub>P</sub> =1.49			(-1.17, -0.42)			DSF <sub>P</sub> =1.53		
P	0%	10%	30%	0%	10%	30%	0%	10%	30%	0%	10%	30%
Test 1	-0.42	-0.41	-0.39	<b>1.91</b>	<b>32.44</b>	<b>136.29</b>	-0.94	-0.97	-0.65	1.27	<b>2.68</b>	<b>5.78</b>
Test 2	-0.41	-0.40	-0.40	1.34	<b>31.76</b>	<b>137.10</b>	-0.91	-0.93	-0.86	0.62	<b>3.52</b>	<b>4.88</b>
Test 3	-0.34	-0.34	-0.34	1.22	<b>33.12</b>	<b>139.32</b>	-0.56	-0.47	<b>-0.19</b>	1.14	<b>2.62</b>	<b>4.71</b>
Test 4	-0.35	-0.35	-0.36	0.69	<b>32.47</b>	<b>136.04</b>	-0.99	-0.99	-0.89	0.53	<b>3.54</b>	<b>4.93</b>
Test 5	-0.37	-0.37	-0.38	0.41	<b>32.70</b>	<b>136.51</b>	-0.88	-0.84	-0.81	0.31	<b>2.53</b>	<b>4.62</b>
Test 6	-0.41	-0.40	-0.39	0.80	<b>33.66</b>	<b>139.28</b>	-0.69	-0.60	<b>0.06</b>	0.82	<b>2.52</b>	<b>4.93</b>
Test 7	-0.39	-0.39	-0.36	0.68	<b>32.77</b>	<b>137.29</b>	-0.91	-0.94	-0.78	0.97	<b>3.18</b>	<b>4.69</b>
Test 8	-0.36	-0.36	-0.37	0.61	<b>32.22</b>	<b>136.28</b>	-0.92	-0.87	-0.70	0.69	<b>3.55</b>	<b>5.04</b>
Test 9	-0.37	-0.39	-0.40	1.15	<b>32.40</b>	<b>137.05</b>	-0.68	-0.63	-0.77	1.02	<b>2.48</b>	<b>4.70</b>
Test 10	-0.43	-0.44	-0.45	1.25	<b>31.63</b>	<b>134.34</b>	-0.93	-0.67	-0.48	1.00	<b>3.01</b>	<b>4.70</b>
Det Rate	0%	0%	0%	10%	100%	100%	0%	0%	20%	0%	100%	100%
	POINT C						POINT D					
	Nair <i>et al.</i> (2006)			Method 2			Nair <i>et al.</i> (2006)			Method 2		
Threshold	(-0.16, 1.43)			DSF <sub>P</sub> =1.47			(-1.73, 1.37)			DSF <sub>P</sub> =1.53		
P	0%	10%	30%	0%	10%	30%	0%	10%	30%	0%	10%	30%
Test 1	0.05	-0.08	<b>-0.31</b>	1.27	1.39	<b>1.92</b>	-0.98	-0.96	-0.91	1.27	<b>1.63</b>	<b>2.69</b>
Test 2	0.92	0.92	0.68	0.62	0.93	<b>1.69</b>	-0.98	0.63	-0.67	0.62	0.88	1.51
Test 3	0.91	0.91	0.72	1.14	1.16	<b>2.22</b>	0.05	0.15	-0.41	1.14	1.17	<b>2.07</b>
Test 4	0.79	0.84	0.94	0.53	0.89	<b>1.78</b>	-0.99	-0.98	0.98	0.53	1.25	<b>2.03</b>
Test 5	0.84	0.87	0.83	0.31	0.59	<b>1.82</b>	0.35	0.22	-0.50	0.31	1.33	<b>2.33</b>
Test 6	0.82	0.87	0.88	0.82	1.15	<b>1.89</b>	0.23	-0.01	-0.51	0.82	1.28	<b>2.72</b>
Test 7	0.85	0.60	-0.03	0.97	1.30	<b>2.12</b>	-0.95	-0.94	-0.90	0.97	0.55	<b>1.74</b>
Test 8	0.96	0.97	0.84	0.69	0.75	<b>1.68</b>	-0.96	-0.95	-0.87	0.69	1.12	<b>2.04</b>
Test 9	0.85	0.80	0.54	1.02	1.00	<b>1.72</b>	0.97	0.97	0.97	1.02	1.31	<b>2.33</b>
Test 10	0.31	0.13	<b>-0.27</b>	1.00	0.98	<b>1.84</b>	-0.98	-0.98	-0.90	1.00	1.38	<b>1.92</b>
Det Rate	0%	0%	20%	0%	0%	100%	0%	0%	0%	0%	10%	90%

**Table 2. Results of damage detection for Method 2.**

Data fusion can be achieved through a number of approaches, the most basic would be a local voting process involving the  $m$  nearest neighbors, signaling damage only when indicated by majority, i.e.,

$$\sum_m B \geq \text{floor}\left(\frac{m}{2}\right) + 1 \quad (6)$$

Thus far, the examples presented for Method 1 (Figure 4) demonstrated over 35% false positive rate associated with an isolated sensor node at point D in the presence of noise. To demonstrate the merits of data fusion within the meso-net, this example is repeated with two additional micro-nets introduced in the vicinity of point D: one at 44.1 cm and the other at 46.55 cm from the fixed end. Again all simulated sensor outputs were corrupted by noise (SNR=100:1). Following the application of Method 1, the binary damage report from each mote is fused in the binary voting scheme in Equation 6. As demonstrated in Figure 6, this fusion reduces the false positive rate to some extent, though damage levels must be quite significant before damage is reliably detected. However, by fusing data not only spatially but also temporally, using a repeated series of measurements, false positive rates can be reduced to 10%,

accompanied by a commensurate increase in the detection rate at lower levels of damage. Such temporal averaging can easily be integrated into the proposed network scheme to improve overall performance.

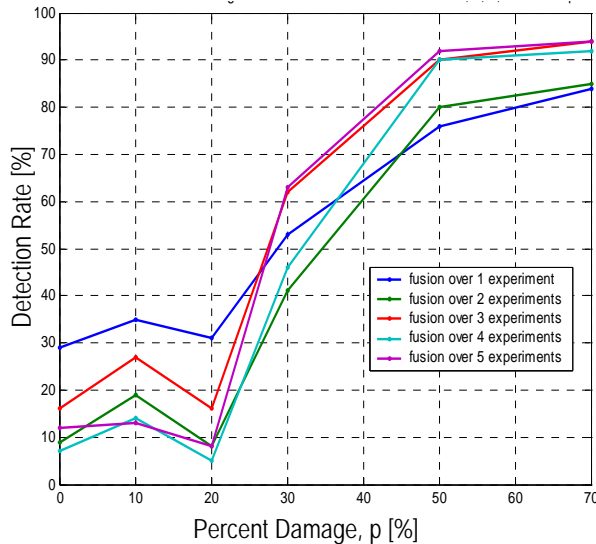


**Figure 6. Data fusion of Method 1 damage reports using three sensors in local vicinity, with temporal averaging.**

## Conclusions

This study overviewed the computational schemes operating within a multi-scale wireless sensor network for structural health monitoring (SHM). The decentralized system identification approaches, both signal-based and time-domain in nature, exploit the heterogeneous sensor array to generate “surrogate inputs” to the damage detection model. The heterogeneous approach was shown to improve detection capabilities at lesser levels of damage, while still operating within the constraints of the wireless platform. In particular, a number of practical advantages over other available techniques were noted for Method 2. Occurrences of false positives and overall detection reliability were further enhanced through the use of data fusion at upper tiers in the network that employ both spatial and temporal averaging.

## Acknowledgements

The authors wish to acknowledge their collaborator Dr. Martin Haenggi at the University of Notre Dame. The financial support of the University of Notre Dame is gratefully acknowledged, as is the support provided by Notre Dame’s Center for Applied Mathematics, through the summer fellowship awarded to the second author.

## References

- Abittan, E. (2006) *A Model-Based Approach for Bridge Structural Health Monitoring Using Wireless Sensor Networks*. Masters Thesis, Department of Electrical Engineering, University of Notre Dame, Notre Dame, IN.
- Doebbling, S.W. and C.R. Farrar (1999) *The State of the Art in Structural Identification of Constructed Facilities*. ASCE Committee on Structural Identification of Constructed Facilities.
- Kijewski-Correa, T., M. Haenggi, P. Antsaklis (2005) “Multi-Scale Wireless Sensor Networks for Structural Health Monitoring,” *Proceedings of SHM-II’05*
- Kijewski-Correa, T., M. Haenggi, P. Antsaklis (2006) “Wireless Sensor Networks for Structural Health Monitoring: A Multi-Scale Approach,” *Proceedings of Structures Congress 2006*, St. Louis.
- Law, S., X. Li, X. Zhu, S. Chan (2005) “Structural Damage Detection from Wavelet Packet Sensitivity,” *Engineering Structures*, **27**, 1339-1348.
- Lynch, J. P., A. Sundararajan, K.H. Law, A.S. Kiremidjian, T. Kenny and E. Carryer (2003) “Embedment of Structural Monitoring Algorithms in a Wireless Sensing Unit,” *Structural Engineering and Mechanics*, **15**, 285-297.
- Lynch, J.P., A. Sundararajan, K.H. Law, A.S. Kiremidjian and E. Carryer (2004) “Embedding Damage Detection Algorithms in a Wireless Sensing Unit for Operational Power Efficiency,” *Smart Materials and Structures*, **13**, 800-810.
- Nair, K.K., A.S. Kiremidjian, and K.H. Law (2006) “Time Series-Based Damage Detection and Localization Algorithm with Application to the ASCE Benchmark Structure,” *Journal of Sound and Vibration*, **291**(1-2), 349-368.
- Sohn, H. and C.R. Farrar. (2001) “Damage Diagnosis Using Time Series Analysis of Vibration Signals,” *Smart Materials and Structures*, **10**(3), 446-451.
- Straser, E. G. and A.S. Kiremidjian (1998) *A Modular, Wireless Damage Monitoring System for Structures*. John A. Blume Earthquake Engineering Center, Department of Civil and Environmental Engineering, Stanford University, Report No. 128.
- Zou, Y., L. Tong and G.P. Steven (2000) “Vibration-Based Model-Dependent Damage (Delamination) Identification and Health Monitoring for Composite Structures – A Review,” *Journal of Sound and Vibration*, **230**, 357-378.